# Impact of delays on the synchronization transitions of modular neuronal networks with hybrid synapses

Cite as: Chaos **23**, 033121 (2013); https://doi.org/10.1063/1.4817607
Submitted: 10 May 2013 . Accepted: 20 July 2013 . Published Online: 05 August 2013

Chen Liu, Jiang Wang, Haitao Yu, Bin Deng, Xile Wei, Kaiming Tsang, and Wailok Chan

# Impact of delays on the synchronization transitions of modular neuronal networks with hybrid synapses

Chen Liu,[1] Jiang Wang,[1,a)] Haitao Yu,[1] Bin Deng,[1] Xile Wei,[1] Kaiming Tsang,[2] and Wailok Chan[2]
[1]*School of Electrical Engineering and Automation, Tianjin University, Tianjin 300072, People's Republic of China*
[2]*Department of Electrical Engineering, The Hong Kong Polytechnic University, Kowloon, Hong Kong*

(Received 10 May 2013; accepted 20 July 2013; published online 5 August 2013)

The combined effects of the information transmission delay and the ratio of the electrical and chemical synapses on the synchronization transitions in the hybrid modular neuronal network are investigated in this paper. Numerical results show that the synchronization of neuron activities can be either promoted or destroyed as the information transmission delay increases, irrespective of the probability of electrical synapses in the hybrid-synaptic network. Interestingly, when the number of the electrical synapses exceeds a certain level, further increasing its proportion can obviously enhance the spatiotemporal synchronization transitions. Moreover, the coupling strength has a significant effect on the synchronization transition. The dominated type of the synapse always has a more profound effect on the emergency of the synchronous behaviors. Furthermore, the results of the modular neuronal network structures demonstrate that excessive partitioning of the modular network may result in the dramatic detriment of neuronal synchronization. Considering that information transmission delays are inevitable in intra- and inter-neuronal networks communication, the obtained results may have important implications for the exploration of the synchronization mechanism underlying several neural system diseases such as Parkinson's Disease. © *2013 AIP Publishing LLC*. [http://dx.doi.org/10.1063/1.4817607]

**Synchronization processes are commonly thought to be considerable important in the neural system, which play a critical role in the mechanism of information communication within different brain areas. Recently, the phenomenon of synchronization transitions in excitable neuronal systems has been investigated extensively, but mostly based on simple neuronal networks companied with a single synaptic form. Besides intrinsic dynamics of neurons are decisive critical elements in the exploration of the synchronization, complex pattern of connectivity strong affects the collective dynamics of the whole neuronal networks. From latest developments of the quantitative analysis of complex neuronal networks, it has demonstrated some common features existing in the brain's structural and functional systems, such as modularity. Based on the coexistence of the electrical and chemical synapses and ubiquity of the information transmission delay, consequently, this paper mainly investigate the corresponding impacts on the synchronization transitions in hybrid-synaptic modular neuronal network. Numerical simulations show that the dependence of the synchronization transitions on the information transmission delay, the probability of electrical synapses, coupling strength, the rewiring probability of the small-world subnetwork, and even the number of subnetworks are attractive. Hence, it may become a thorough understanding of the synchronization mechanism, further helping to reveal the mechanism of the neurological diseases, such as the epilepsy and Parkinson's disease.**

## I. INTRODUCTION

Synchronization of complex clustered networks has increasingly attracted considerable attentions in recent years.[1–3] Especially in the neural system, synchronous activities are commonly observed[4–6] and revealed to be associated not only with various normal brain functions,[7–9] such as cognitive functions; but also with pathological brain states,[10–12] like the epilepsy[13] and Parkinson's disease.[14,15] It is reported that synchronization is a significant mechanism in processing information within different brain areas, where synchronization often manifests an emerging phenomenon of a population of dynamically interacted units.[16,17] Till now, synchronization of the neuronal network has been extensively explored. Plenty of results[18–22] suggest that small-world,[23–25] scale–free,[26,27] and weighted networks[28,29] are generally more synchronizable than regular networks. Interestingly, the cortical neuronal network often shows the modularity feature with its complex connectivity.[30–32] Thus, it is necessary to study the dynamics of modular neuronal networks to understand the brain function better.

Recently, a tremendous amount of progress demonstrate that some common features of complex networks are found in the brain's structural and functional systems, such as small-world topology, highly connected hubs, and modularity.[33–36]

a)Author to whom correspondence should be addressed. E-mail: jiangwang@tju.edu.cn. Fax/Tel: 86-22-27402293

 

As is well known, the small-world feature generally refers to neuronal networks having a high clustering coefficient and a relatively short minimum path length on average between each pair of its nodes.[23,37,38] Models of neural systems with small-world coupling can display enhanced signal-propagation speed, computational power, and synchronizability.[39] Moreover, on the basis of the small-world feature, within the same module, neurons are always densely connected to other neurons with internal connectivity, and sparsely connected to neurons in other modules with external connectivity.[40–43] Furthermore, previous studies have revealed the modularity of the cortical neuronal networks in the brain[35] as well as the synchronization phenomenon in a clustered neuronal network consisting of subnetworks.[44–46]

In the neuronal systems, two different types of synapses may occur in the coupling between neurons, the electrical and chemical ones.[47–51] It is reported that electrical synapses is the gap-junctional coupling, which may cause an immediate physiological response of the adjacent neurons. Its strength linearly depends on the difference between the membrane potentials,[52,53] while the chemical synapse, described by a nonlinear function, is mediated by the exchange of neurotransmitters from the pre- to the post-synaptic neuron. It can only act once the presynaptic neuron membrane achieves a certain action potential.[54] Recently, the synchronous dynamical behaviors of the neuronal systems with two types of synapses have attracted more and more attention. Kopell *et al.* found that both electrical and chemical synapses play the different-but-complementary roles in the synchronization of neuronal networks.[55] Baptista *et al.* further combined two types of the synapses to study the process of synchronization and the information production.[56]

Due to the finite speed of action potential propagating across neuron axons and time lapses occurring by both dendritic and synaptic processes, it is always inevitable for the information transmission delays in neural systems.[57–59] Various studies have shown that the information transmission delays may induce multiple stochastic resonances in neuronal networks.[60] Moreover, it is reported that delay can facilitate the neuronal synchronization or destabilize synchronous states, therefore resulting in various spatiotemporal patterns irrespective of the excitatory and inhibitory chemical synapses.[39,61–64] Nevertheless, there are still little works on studying the dependence of synchronization transitions in modular networks with electrical and chemical hybrid synapses on delays.

Consequently, the present study explores the impacts of the information transmission delay and the probability of electrical synapses on the synchronization transitions in modular neuronal networks. Rulkov map-based models are used to construct a model of modular neuronal network composed of subnetworks, where one of them is taken as a hub module directly connecting to other subnetworks. Accordingly, the remainder of this paper is organized as follows. Section II describes the model of the modular neuronal networks with hybrid electrical and chemical synapses. In Sec. III, the impacts of the information transmission delays and the various network parameters on the synchronization transitions in modular neuronal networks are investigated. Finally, a brief conclusion of our work is given in Sec. IV.

## II. MODEL AND METHOD

In order to explore the synchronous activities in the modular neuronal network, the topology structure and mathematical description of the considered network are given in this section. For simplicity, assume that there exist $M$ subnetworks with small-world topology structures, and each subnetwork

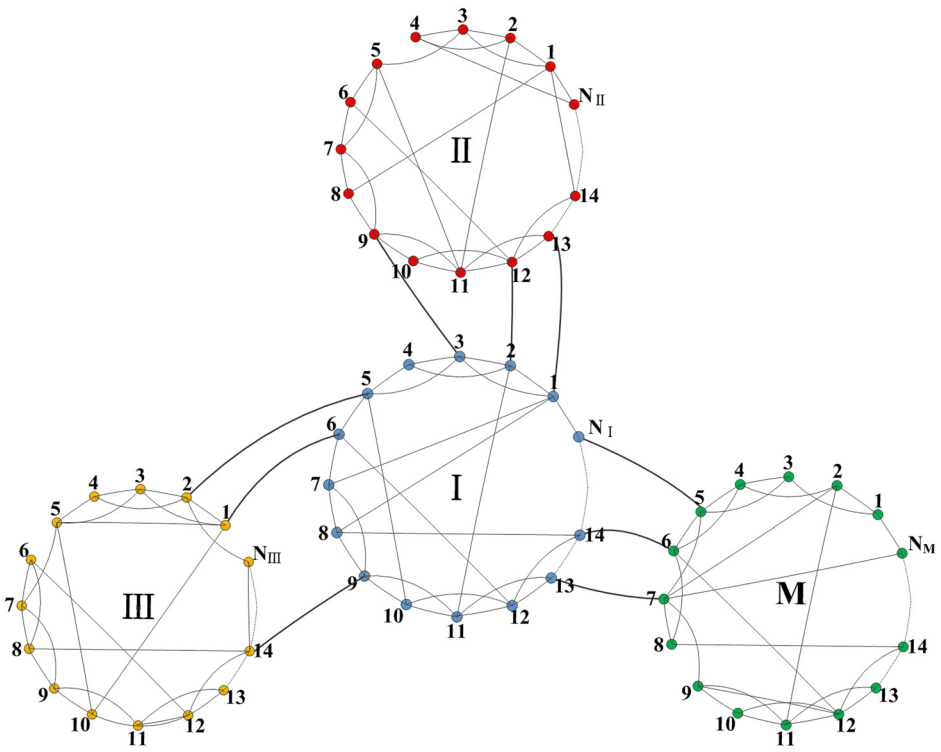


FIG. 1. The illustration of the modular neuronal network with $M$ subnetworks. Within a module, $N_I(I = \mathrm{I}, \mathrm{II}, ..., M)$ nodes are connected to each other based on the small-world property; modules are only sparsely connected. Every node represents a neuron.

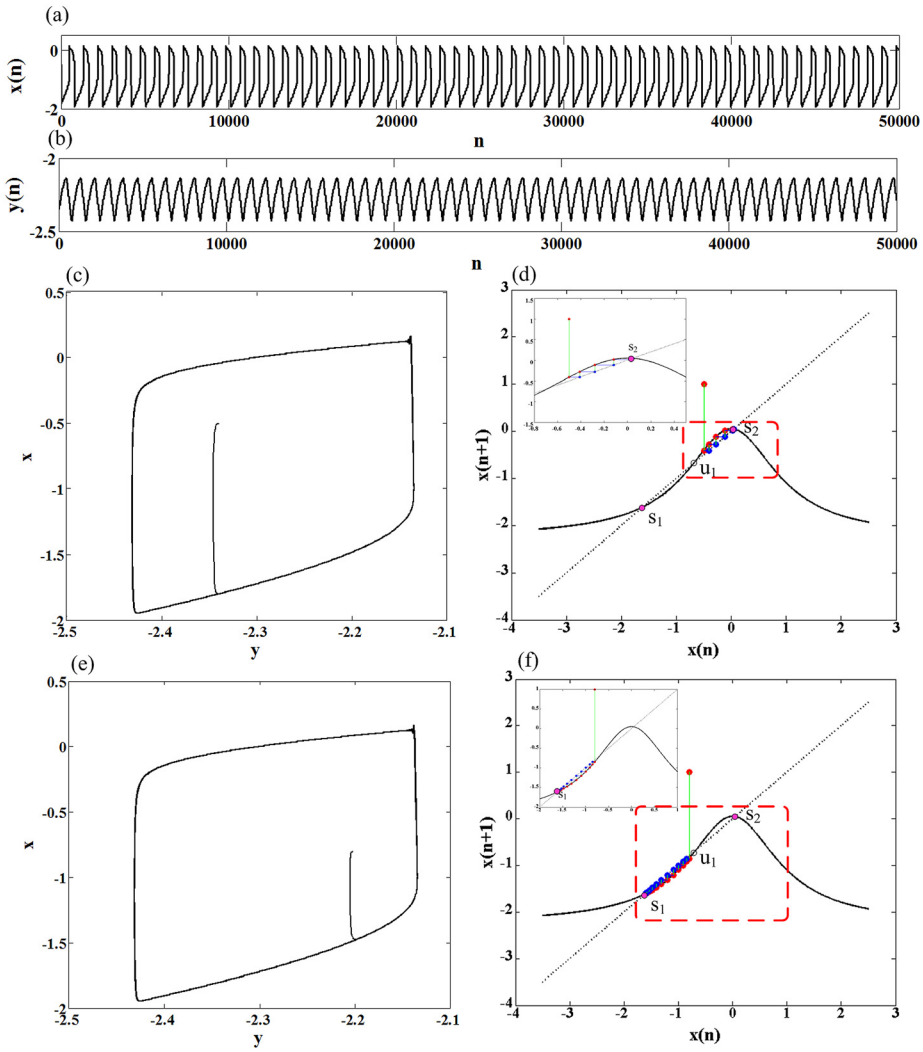


FIG. 2. (a) Time evolution of the fast variable in Rulkov model along a periotic spiking orbit. (b) The corresponding time evolution of the slow variable. (c) Phase plane diagram of the Rulkov model. A stable limit circle stands for a periotic spiking pattern. States of the fast subsystem of the Rulkov model will eventually converge to the stable fixed point $s_2$. (d) Return map of the same cases as (c). (e) Phase plane diagram of the Rulkov model. States of the fast subsystem of the Rulkov model will eventually converge to the stable fixed point $s_1$. (f) Return map of the same cases as (e). Parameter values are $\alpha = 2.3$, and $\beta = \gamma = 0.001$. The initial state falls into the left region divided by the value of the stable fixed point $s_2$.

containing the $N$ nodes; one module in the neural network is randomly chosen as a hub module; then some pairs of nodes from the hub module and other subnetworks are randomly chosen and then linked with the interconnection probability $P$.

Fig. 1 shows an illustration of the modular neuronal network with $M$ subnetworks, where every node represents a neuron. To obtain a small-world subnetwork, following random rewiring procedure proposed by Watts and Strogatz is taken into account.[23] A ring-like network is regarded as an original neuronal network with regular connectivity comprising $N$ nodes, each connected to its $K = 6$ nearest neighbors. With probability $rp$, each edge is rewired at random. By increasing the probability $rp$, the architecture of the network can be tuned between two extremes, regular ($rp = 0$) and random ($rp = 1$) networks. For $0 < rp < 1$, the resulting network may have small-world property. Initially, a modular neuronal network of small-world subnetworks with pure chemical synapses could be modeled. By increasing probability of electrical synapses $p$ with respective to the existing edges within the subnetworks, the neuronal networks with hybrid synapses can be established. Subnetworks is changed from pure chemical synapses subnetworks to hybrid synapses subnetworks with $p$, while the sparse chemical coupling between subnetworks remains invariable. The rewiring probability, coupling strength and the number of the subnetworks are also the important parameters to be investigated in this paper. In order to connect the different subnetworks to form a whole modular network, the interconnection probability $P$ is set to 0.005.

In order to capture the main dynamical features of the more complex time-continuous neuronal models and also ensure a numerical effectiveness to simulate the evolution of the individual neuron's dynamics, two-dimensional map proposed by Rulkov is used to simulate the dynamics of individual neuron in each subnetwork.[65,66] Spatiotemporal dynamics of the modular network with information transmission delay and hybrid synapses is governed by the following iteration equations:

$$\begin{aligned} x_{I,i}(n+1) &= \frac{\alpha}{1 + x_{I,i}^2(n)} + y_{I,i}(n) + I_{I,i}^{syn}(n), \\ y_{I,i}(n+1) &= y_{I,i}(n) - \beta x_{I,i}(n) - \gamma, \end{aligned} \tag{1}$$

where $n$ is the discrete time index, $(I, i)$ is the $i$th neuron ($i = 1, 2 \ldots N$) in the $I$th subnetwork ($I = 1, 2 \ldots M$); $x$ and $y$ are fast and slow dynamical variables of the map denoting the transmembrane voltage and the variation of the ion concentration, respectively. The slow evolution of $y$ is due to small values of the parameters $\beta = 0.001$ and $\gamma = 0.001$, whereas parameter $\alpha$ determines main dynamical properties of an isolated Rulkov neuron. According to Ref. 66, if $\alpha < 2$, all the

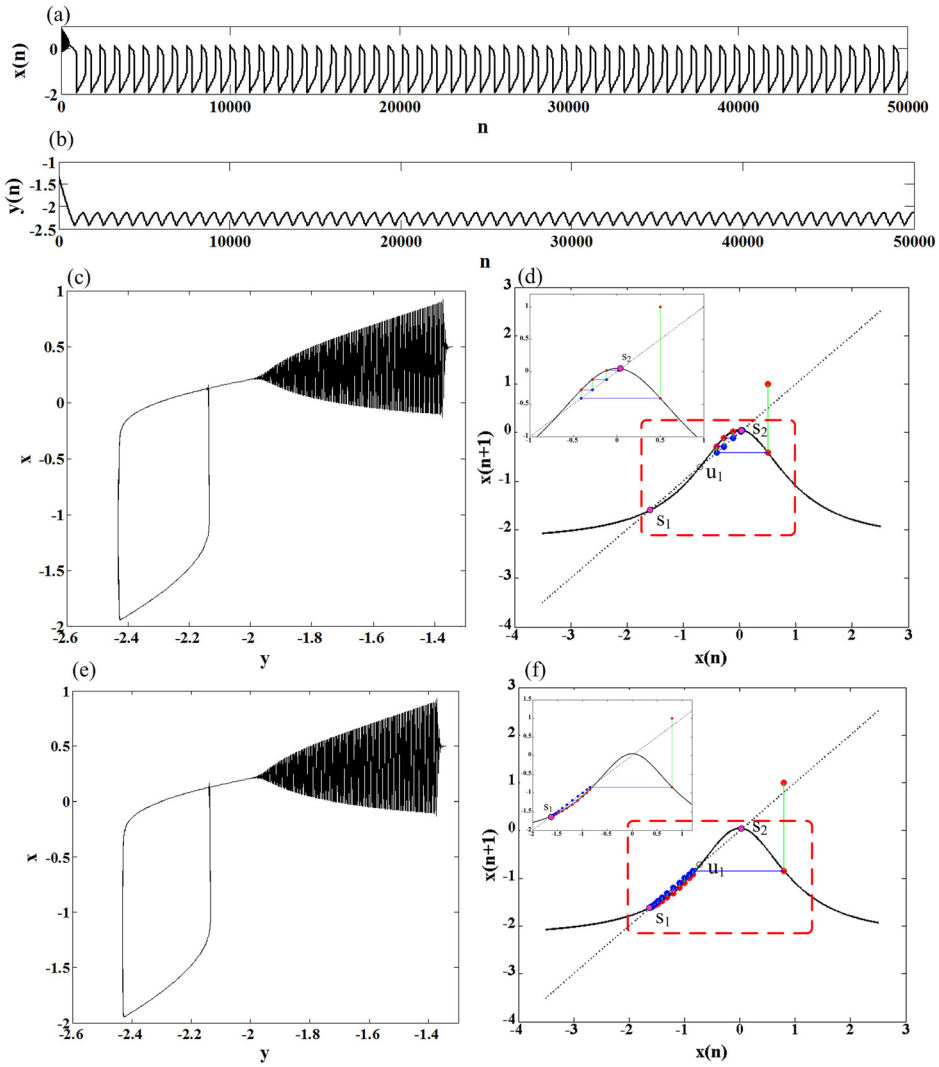


FIG. 3. (a) Time evolution of the fast variable in Rulkov model along a periotic spiking orbit. (b) The corresponding time evolution of the slow variable. (c) Phase plane diagram of the Rulkov model. A stable limit circle stands for a periotic spiking pattern. States of the fast subsystem of the Rulkov model will eventually converge to the stable fixed point $s_2$. (d) Return map of the same cases as (c). (e) Phase plane diagram of the Rulkov model. States of the fast subsystem of the Rulkov model will eventually converge to the stable fixed point $s_1$. (f) Return map of the same cases as (e). Parameter values are $\alpha = 2.3$, and $\beta = \gamma = 0.001$. The initial state falls into the right region divided by the value of the stable fixed point $s_2$.

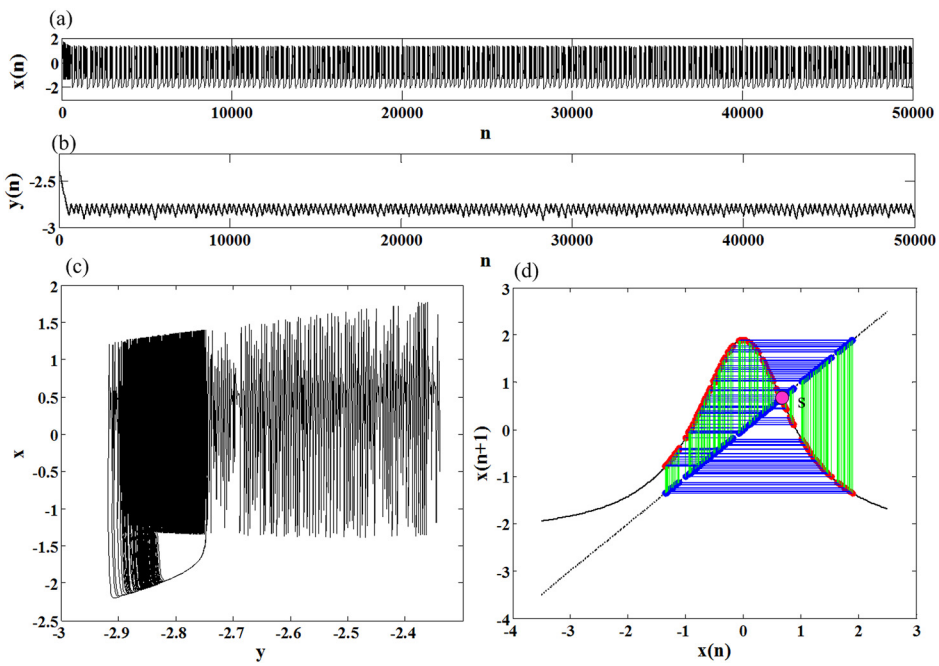


FIG. 4. (a) Time evolution of the fast variable in Rulkov model along a bursting orbit. (b) The corresponding time evolution of the slow variable. (c) An orbit of the chaotic Rulkov map in the phase plane diagram. (d) Return map of the same cases as (c) Parameter values are $\alpha = 4.15$ and $\beta = \gamma = 0.001$.

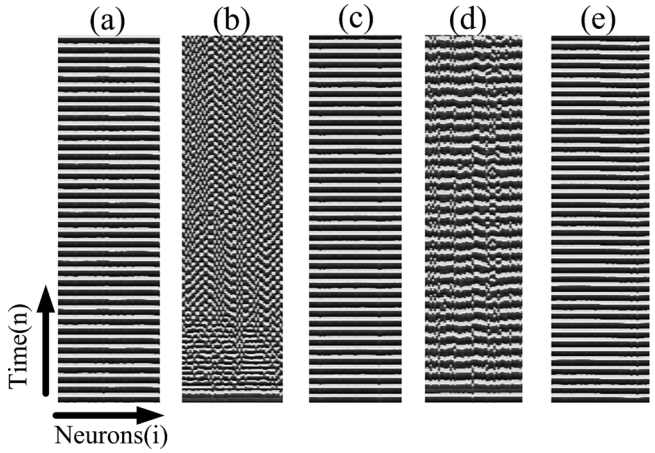


FIG. 5. Space-time plots obtained for different information transmission delays in the modular neuronal network with the electrical synapses. From (a) to (e), information transmission delay $\tau$ equals to 0, 400, 750, 1150, and 1450, respectively. Other parameters are $\varepsilon_{in} = 0.01$, $\varepsilon_{ex} = 0.005$, and $rp = 0.1$. Note the emergence of synchronization in panels (a), (c), and (e).

neurons in the modular network are situated in their own steady state $[x^* = -1, y^* = -1 - (\alpha/2)]$, whereas if $\alpha > 2$, the fast variable $x$ of the map-based neuron displays spiking-bursting and oscillatory patterns. In order to further explore the impact of the bifurcation parameter $\alpha$ on the characteristics of the Rulkov's model, an unimodal first return map of the fast subsystem is depicted in Figs. 2(d) and 2(f). Here, we approximately set the value of the slow variable $y = -2.25$. First, Figs. 2 and 3 show the case of $\alpha = 2.3$, where there exist a stable-unstable fixed point pair, labeled $s_1$ and $u_1$ and another stable fixed point $s_2$. Obviously, random initial state can always converge to one of the stable fixed points, rather than the unstable fixed point $u_1$. Interestingly, the entire return map plane can be divided into two segments by the unstable fixed point. When the random initial state $x$ is higher than the value of the unstable fixed point $u_1$, the state will converge to stable fixed point $s_2$, as shown in Figs. 2(d) and 3(d); otherwise stable fixed point $s_1$, seen in Figs. 2(f) and 3(f). Thus, in the case of $\alpha = 2.3$, the Rulkov's model can be regarded as a periodic system. The evolutions of the membrane potential $x$ and its slow recovery variable $y$ display its periodic dynamical characteristics. It can be easily found that several interesting differences between Figs. 2 and 3. If the initial states $x$ fall into the right segment of the stable fixed point $s_2$, a kind of similar initial chaotic property will emerge. However, since there still exists a stable limit circle as shown in the phase image of Figs. 3(c) and 3(e), the overall periodicity characteristics remain unchanged.

Furthermore, another typical characteristic of the Rulkov's model is shown in the case of a sufficiently high $\alpha$ ($\alpha \in [4.1, 4.4]$), where an individual map can exhibit chaotic bursts. As shown in Fig. 3, increase of the $\alpha$ will make the first return map shift up, which induce the disappearance of the fixed point pair $s_1$ and $u$ through the saddle-node bifurcation. In Fig. 3, for $\alpha = 4.15$, it can be obviously seen that different random initial states could not always converge to remaining fixed, implying that the firing orbits are no longer periodic, but chaotic. This paper aims to explore the complete synchronization of the modular neuronal network, thus here $\alpha = 2.3$ for which individual neuron exhibiting simple single-burst excitations.[66]

In Eq. (1), $I_{I,i}^{syn}(n)$ is the synaptic current term described as follows:

$$\begin{aligned} I_{I,i}^{syn}(n) = {} & \varepsilon_{in} \sum_{j=1}^{N} A_{CI}(i,j)(x_{I,i}(n) - v_{I,i})\Gamma(x_{I,j}(n)) \\ & + \varepsilon_{in} \sum_{j=1}^{N} A_{EI}(i,j)(x_{I,i}(n) - x_{I,j}(n-\tau)) \\ & + \varepsilon_{ex} \sum_{J=1}^{M} \sum_{j=1}^{N} B_{I,J}(i,j)(x_{J,i}(n) - v_{J,i})\Gamma(x_{J,j}(n)), \end{aligned} \quad (2)$$

where $\varepsilon_{in}$ and $\varepsilon_{ex}$ represent the coupling strength within each subnetwork and between different subnetworks in the whole system, respectively. $v$ represents the synaptic reversal

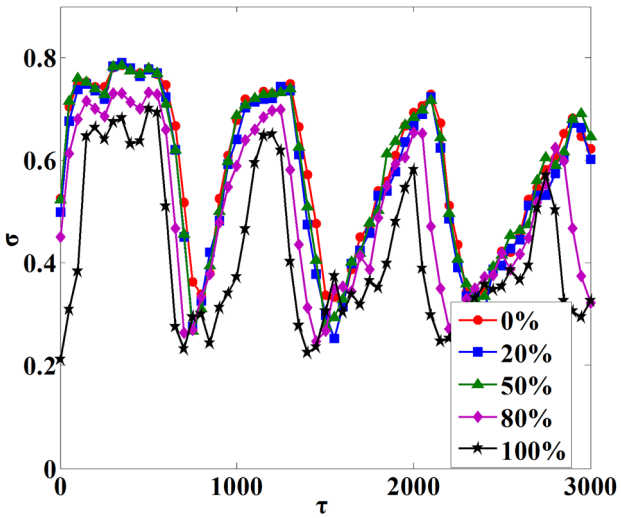


FIG. 6. Dependence of synchronization parameter $\sigma$ on the information transmission delays $\tau$ for several electrical synapses probabilities $p$ in the different neuronal networks. Calculation of $\sigma$ is obtained from the whole modular neuronal network. Other parameters are $\varepsilon_{in} = 0.01$, $\varepsilon_{ex} = 0.005$, and $rp = 0.1$. It can be seen that certain values of $\sigma$ significantly facilitate spatiotemporal synchronization of excitatory fronts on the modular small-world neuronal networks with hybrid synapses.

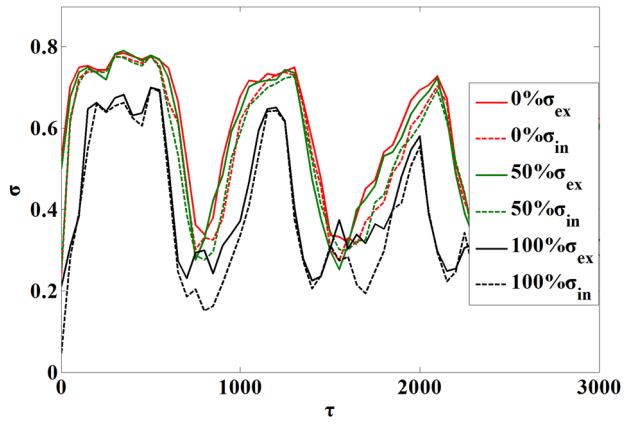


FIG. 7. The comparison of the calculation results of $\sigma$obtained from the single module of the whole neuronal network and the whole modular neuronal system. Other parameters are $\varepsilon_{in} = 0.01$, $\varepsilon_{ex} = 0.005$, and $rp = 0.1$. The synchronization within each subnetwork seems much easier to be achieved, irrespectively of the probability of the electrical coupling.

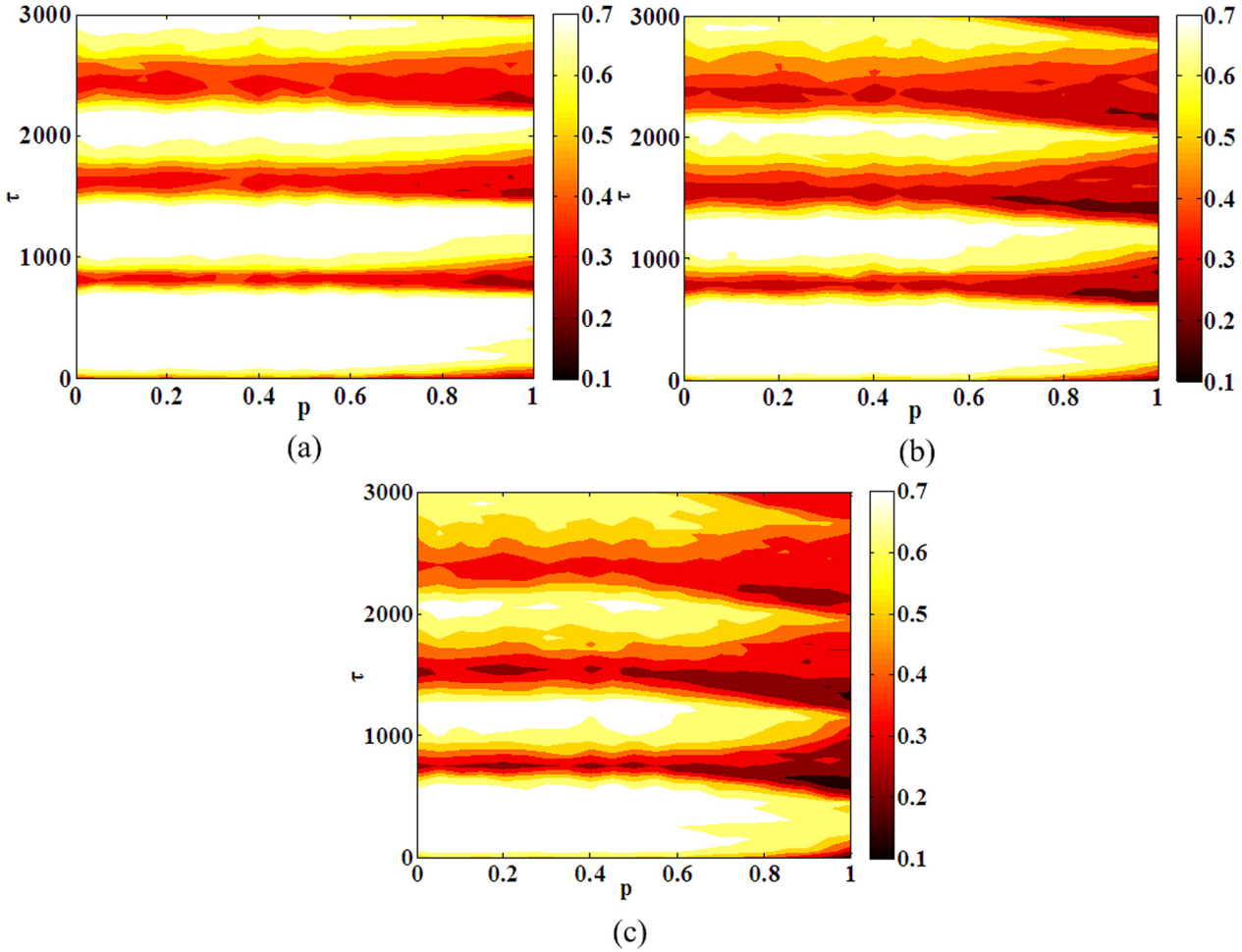


FIG. 8. Dependence of synchronization parameter $\sigma$ both on the information transmission delays $\tau$ and the electrical synapses' probabilities $p$ for different coupling strength. Synchronization transitions can appear as the information transmission delay increased. And above a certain threshold, the synchronous behaviors are greatly enhanced. (a) $\varepsilon_{in} = 0.005$, (b) $\varepsilon_{in} = 0.01$, and (c) $\varepsilon_{in} = 0.015$. Other parameters are $\varepsilon_{ex} = 0.005$ and $rp = 0.1$.

potential, here $v = 1.8$ for excitatory chemical synapses. Moreover, $A_{CI}(i,j) = 1$, if neuron $i$ is chemically coupled to neuron $j$ within subnetwork $I$, and $A_{EI}(i,j) = 1$ if electrical synapse exists between the neuron $i$ and neuron $j$ within subnetwork $I$; otherwise $A_{CI}(i,j) = 0$ and $A_{EI}(i,j) = 0$. $B_{I,J}(i,j) = 1$ if $i$th neuron in the $I$th subnetwork is chemically connected to $j$th neuron in the $J$th subnetwork, and $B_{I,J}(i,j) = 0$ otherwise. Furthermore, the information transmission delay synaptic coupling function is described in the form of the sigmoidal function $\Gamma(x_j) = 1/(1 + \exp\{-\lambda[x_j(n-\tau) - \Theta_s]\})$. Regard $\Theta_s = -1.0$ as a threshold, above which the postsynaptic neuron is affected by the presynaptic one. $\lambda = 30$ is an invariable rate for the onset of the excitation. Here, the information transmission delay $\tau$ among the modular neuronal network is a core variable.

Synchronization degree of the modular neuronal network is quantitatively characterized by a synchronization parameter $\sigma$, which is taken the form of the standard deviation is defined as

$$\sigma = \sqrt{\frac{1}{T}\sum_{n=1}^{T}\sigma(n)},\ \sigma(n) = \frac{1}{N}\sum_{i}^{N}[x_{I,i}(n)]^2 - \left[\frac{1}{N}\sum_{i=1}^{N}x_{I,i}(n)\right]^2, \tag{3}$$

where $T$ is the period of numerical integration. It is obvious that the smaller the synchronization parameter $\sigma$, the more synchronous the modular neuronal network from Eq. (3). Hence, $\sigma = 0$ means a completely synchronization. Presented simulation results are averaged over twenty independent runs.

## III. RESULTS

Initially, a modular network consisted of two small-world subnetworks is constructed, wherein all the synapses being chemical, irrespectively within or between the subnetworks. By gradually increasing the probability of the electrical synapses within each subnetwork, the neuronal subnetworks with pure chemical synapses, hybrid synapses, or even pure electrical synapses are shaped, respectively. To investigate the dependence of synchronization transition in the information transmission on time delay, the gradually increasing delay is added into the neuronal system. Obviously, as shown in Fig. 5, the typical space-time plots observed on the modular network for different values of the delay $\tau$ imply that information transmission delay can drastically influence the neuron behaviors, inducing intermittent appearance of synchronization regions. Results presented in

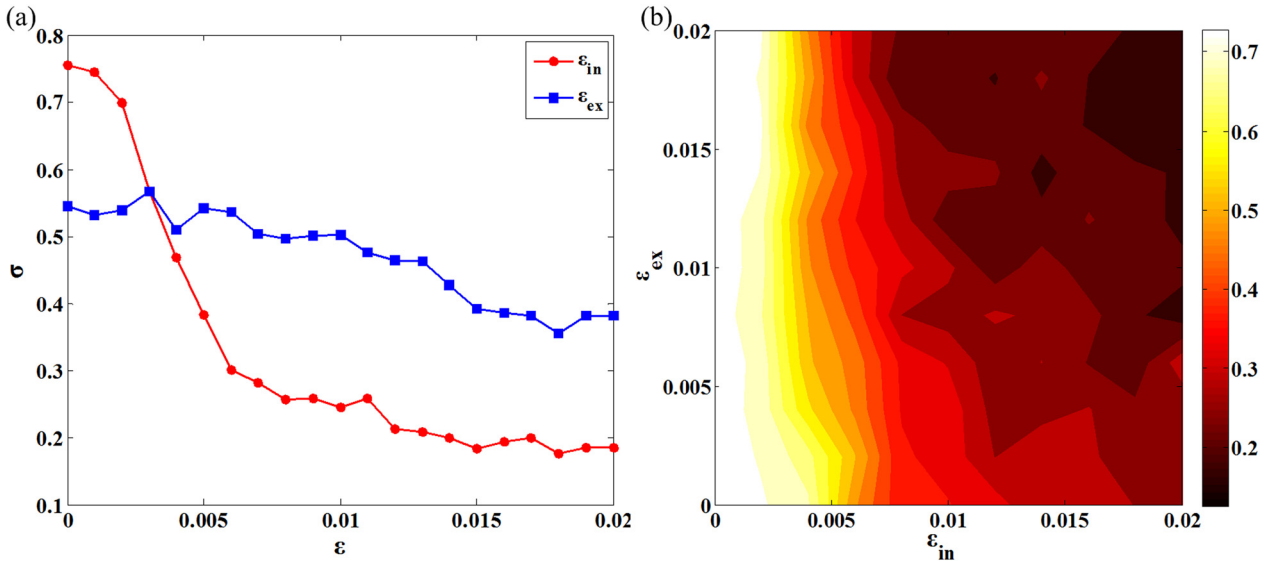


FIG. 9. (a) Dependences of the synchronization parameter $\sigma$ on the intra- and inter- coupling strength in the case of $p = 0.5$. Plots are obtained from the synchronous regions of the modular neuronal network $\tau = 750$. (b) An overall view of the dependences of the synchronization parameter $\sigma$ both on the intra- and inter-coupling strength in the modular neuronal network. The regions of the synchronous activities always emerge in the large coupling strength irrespective of the intra- and inter-synapses. Other parameters are $p = 0.5$ and $\tau = 750$.

Fig. 5(a) indicate that the spatiotemporal dynamics are synchronous in the absence of information transmission delay. However, with information transmission delay increasing, when $\tau$ is 400, the synchrony has been drastically destroyed, as observed in Fig. 5(b), where spatiotemporal activities seem disorder. Nevertheless, it is depicted in Fig. 5(c), synchronous pattern emerges again as $\tau$ further increases to 750, and then again disappears at $\tau = 1150$ and reappears at $\tau = 1450$, as shown in Figs. 5(d) and 5(e), respectively.

In order to quantitatively characterize the synchronization degree of the neurons in hybrid modular networks, the synchronization parameter $\sigma$ is calculated[67] as defined by Eq. (3). From Fig. 6, it can be found that when the synapses within the initial subnetwork are all chemical synapses, there exist several minima of $\sigma$ as $\tau$ gradually increases, which may imply that delays can induce the intermittent transitions of the synchronization emerging in the modular neuronal network. Subsequently, electrical synapses are gradually added into the subnetworks with an increasing percentage of all synapse coupling within the subnetworks. Several lines in the Fig. 6 demonstrated that as the probability of the electrical synapses increases, the synchronization cannot be enhanced obviously until probability exceeds a certain threshold. Evidently, only when more than half of the synapses turn to electrical synapses within the subnetwork, the intermittent synchronization could be improved as the information transmission delay increases. Hence, the probability of the electrical synapses plays a significant role in the synchronization transitions.

More interestingly, it can be seen that if the synchronization parameter $\sigma$ is obtained within the subnetwork, the corresponding results of the effects of the time delay on the synchronous behaviors are presented in Fig. 7. It is easily found that as the electrical synapses increased, the activities of the neurons in each subnetwork also display the more synchronous on the premise that the probability of the electrical synapses exceeding a certain threshold. In addition, it reveals another attractive phenomenon that a higher degree of synchronization within each subnetwork can be obtained by contrasting the values of the $\sigma$ calculated from the local subnetwork with the whole modular network, which are labeled $\sigma_{in}$ and $\sigma_{ex}$, respectively. It may suggest that sparse and weak coupling among the subnetworks may reduce the degree of synchronization. Furthermore, a fascinating exploration will be carried out about the impact of the number of the subnetworks on the whole synchronization, the interesting results being shown in the last two figures.

To make an overall inspection, a two-dimensional parameter space is used to show the dependence of $\sigma$ on both $p$ and $\tau$, as exhibited in Fig. 8. It is obvious that several band-like regions in dark color represent the modular network's high degree of synchronous activities. However, for other information transmission delays outside the dark regions, neuronal synchronization may be unfortunately impaired. Importantly, the regions of synchronization can be expanded and the degree of synchronization can be enhanced when the probability of the electrical synapses is over half. The occurrence of this phenomenon may mainly due to structure of the modular neuronal network. It may result from the fact that only the electrical synapses can induce an immediate physiological response to the adjacent neurons' induced behaviors. Thus, the probability of the electrical synapses needs to achieve a certain threshold to enhance the synchronous activities in the whole neuronal network. Furthermore, the collective activities of the modular network could be turned out to be more synchronous with the coupling strength increasing as shown in Figs. 8(a)–8(c), where the coupling strengths in the subnetworks are 0.005, 0.01, and 0.015, respectively.

This interesting phenomenon attracts us to focus on the stability analysis of synchronous states, here, a numerical

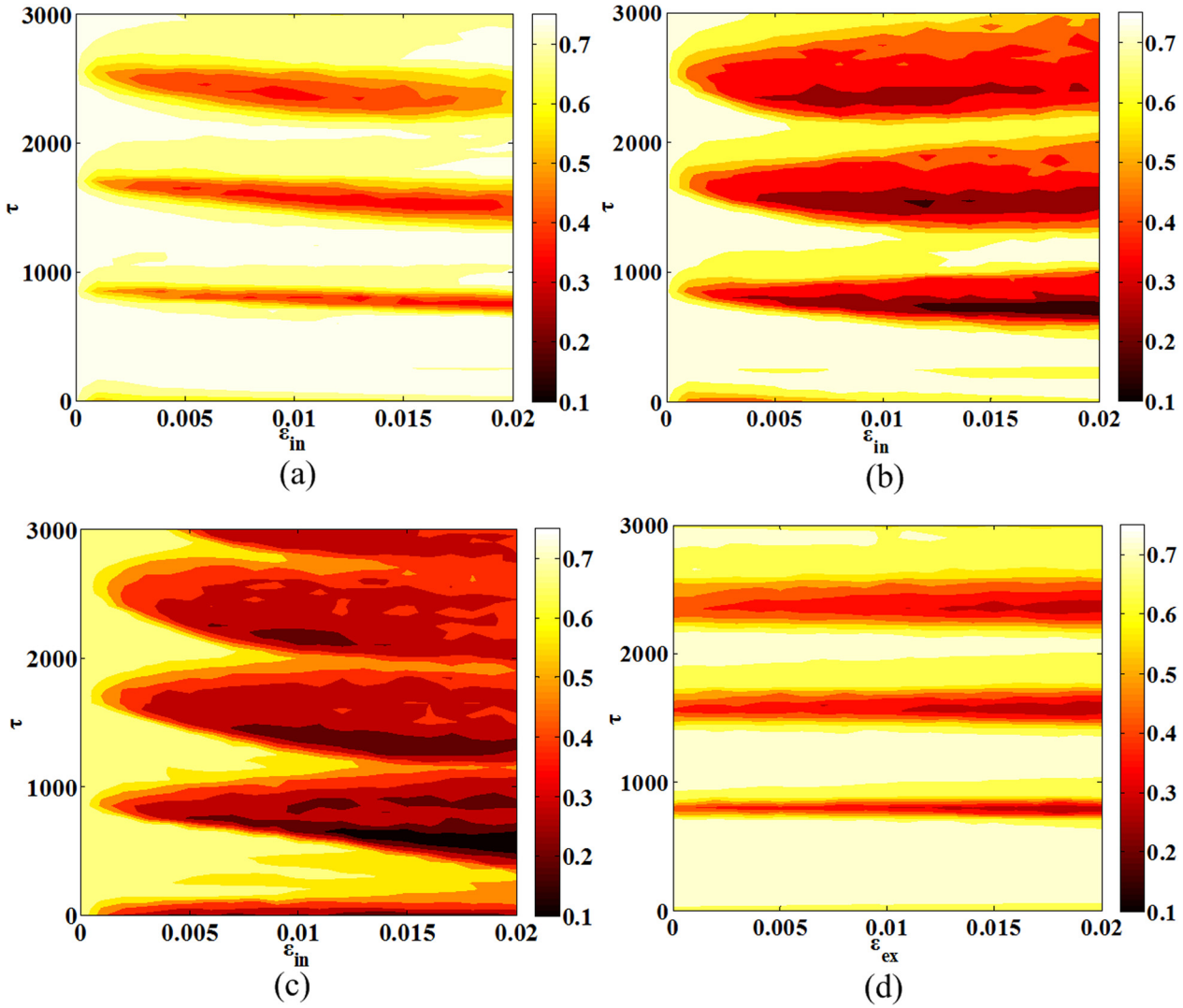


FIG. 10. Dependence of synchronization parameter $\sigma$ both on the information transmission delays $\tau$ and the intra-coupling strength $\varepsilon_{in}$ for the neuronal network with (a) pure chemical synapses (b) fifty percent electrical synapses and fifty percent chemical synapses (c) pure electrical synapses. Other parameters are $\varepsilon_{ex} = 0.005$ and $rp = 0.1$. (d) Dependence of synchronization parameter $\sigma$ both on the information transmission delays $\tau$ and inter-coupling strength $\varepsilon_{ex}$ for the neuronal network with fifty percent electrical synapses and fifty percent chemical synapses. Other parameters are $\varepsilon_{in} = 0.01$ and $rp = 0.1$. With the $\tau$ increasing, the regions of the synchronization appear intermittently. For large coupling strength, synchronous activities emerge more easily. And due to the sparseness of the inter-modules' coupling, the inter-coupling strength seems to be less profound.

result demonstrates our deduction about the large coupling strength maybe inducing a more synchronous state. As shown in the case of the hybrid synapse in Fig. 9, here $p = 0.5$, the dependences of the synchronization parameter $\sigma$ on the intra- and inter-coupling strengths both indicate that the synchronization is stable. The plots in Fig. 9(a) indicate not only for a certain inter-coupling strength $\varepsilon_{ex}$ between the modules, as the intra-coupling strength $\varepsilon_{in}$ increased, the synchronization is enhanced and stabilized gradually; but for a certain intra-coupling strength $\varepsilon_{in}$, the changes of the synchronization are less obvious. In order to gain more insights into the competing interactions of the intra- and inter-coupling strengths, a comprehensive view of their impacts on the synchronization is given in Fig. 9(b). It can be evidently found that for a small $\varepsilon_{in}$, the modular neuronal network exposes a weak synchronization, which implies that two non-synchronous subnetworks is hard to achieve the synchronous states only by adjusting $\varepsilon_{ex}$. However, if the neurons in each subnetwork are initially synchronous, the increasing $\varepsilon_{ex}$ will play an advantageous role in the promoting the whole synchronization. In addition, for any $\varepsilon_{ex}$, $\varepsilon_{in}$ always has a better influence; especially in the case of the large $\varepsilon_{ex}$, the clusters can display an increasing synchronous pattern as $\varepsilon_{in}$ increases. Similar conclusions can be obtained from the modular neuronal network with other proportions of electrical and chemical synapses.

Figs. 10(a)–10(c) show the impacts of the intra-coupling strength $\varepsilon_{in}$ on the synchronization in the case of the three different networks: a network of pure chemical synapses, a hybrid network of hybrid synapses, and a network of pure electrical synapses. In the hybrid modular neuronal network (see the Fig. 10(b)), the obvious phenomenon of the intermittent synchronization emerges again when the intra-coupling strength is large enough. Interestingly, as the coupling

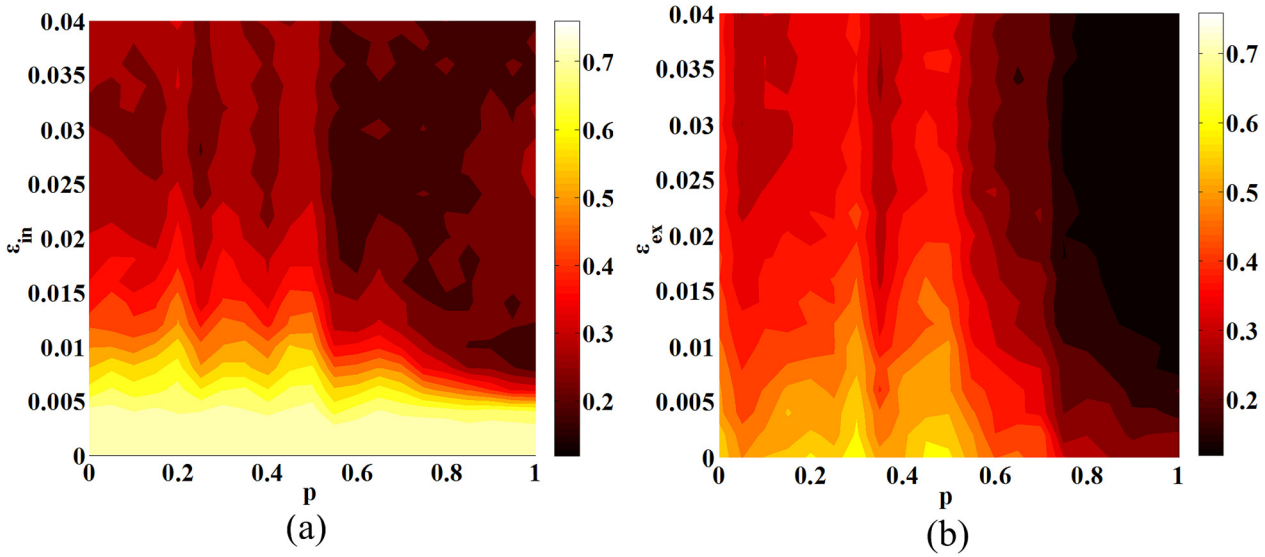


FIG. 11. (a) Dependence of synchronization parameter $\sigma$ both on the intra-coupling strength $\varepsilon_{in}$ and electrical probabilities $p$ for the information delay $\tau = 750$. The increasing intra-coupling strength can obviously promote the synchronization of the neurons. Other parameters are $\varepsilon_{ex} = 0.005$ and $rp = 0.1$. (b) Dependence of synchronization parameter $\sigma$ both on the inter-coupling strength $\varepsilon_{ex}$ and electrical probabilities $p$ for the information delay $\tau = 750$. The increasing inter-coupling strength seems has less effect on the enhancement of the synchronization. Other parameters are $\varepsilon_{in} = 0.01$ and $rp = 0.1$.

strength within the subnetwork increases, the regions of the synchronization gradually turn broad, where the synchronous patterns can be regarded to be stable. Synchronization of the modular neuronal network may not disappear anymore as its coupling strength increases. Similar results are obtained from the networks of the single type of synapses no matter chemical synapses as shown in Fig. 10(a) or electrical synapses as shown in Fig. 10(c). Additionally, it can be found that collective activities of the network become more synchronous with the electrical synapses being gradually added into the subnetwork. For the pure electrical subnetwork, band-like regions of the synchronization become broad enough, that is to say, some certain information transmission delays may not easily destroy the synchronization of the modular network any more. Furthermore, it can be seen that, due to the sparse synapses connecting the individual subnetworks, inter-coupling strength cannot induce a significant impact on the synchronization (see Fig. 10(d)).

To conduct a further study about the dependence of synchronization lever $\sigma$ on coupling strength and the probability of the electrical synapses in the modular network, synchronization parameters are calculated for various probabilities of the electrical synapses with intra- and inter-coupling strengths increasing, respectively, as shown in the Figs. 11(a) and 11(b). Here, the information transition delay is chosen as $\tau = 750$, which can enhance synchronous activities in the neuronal network, as shown in Fig. 6. It is shown that the synchronization will be promoted in the case of large probability of the electrical synapses and strong intra-coupling strength in Fig. 11(a). However, a different result is obtained in Fig. 11(b), where inter-coupling strength seems have a less profound effect on the synchronization transition. It may imply that sparse chemical synapses could not induce a significant change of the synchronous behaviors in the whole modular neuronal network. Moreover, it may further conclude that the synchronization will be enhanced dramatically, only if the probability of the electrical synapses reaches a certain threshold.

Furthermore, in the exploration of the dependence of synchronous activities on the coupling strength, the intra-coupling strength is divided into two parts. Fig. 12 gives the combined dependence of the synchronization on the chemical coupling strength and electrical coupling strength. From (a) to (d), the probabilities of the electrical synapses in the modular neuronal network are 20%, 50%, 70%, and 80%. It is obviously found that the increasing electrical coupling will gradually enhance the synchronization of the neuronal system. Additionally, as the electrical synapses' dominance becomes more apparent, the coupling strength of the electrical synapses plays a more important role in the synchronization transitions. As shown in Figs. 12(a) and 12(b), when the minority electrical coupling exists in the subnetworks, its coupling strength can hardly induce the improvement of the synchronization. In this case, the chemical synapses turn out to be more significant instead, where suitable chemical coupling strength may greatly facilitate synchronous behaviors in the whole modular neuronal network. However, when the ratio of the electrical and chemical coupling increases to 7:3, as shown in Fig. 12, the combined effects on the synchronous activities of the neurons become evident, where the coupling strengths of the two types of the synapses simultaneously make an impact on the synchronization of the modular network to a similar degree. Moreover, only if a serious imbalance between the numbers of two types of the synapses appears once more as exhibited in Fig. 12(d), due to the majority of the electrical synapses, the synchronization of the whole neuronal network largely depends on the electrical coupling strength. Obviously, synchronous behaviors centrally occurred on the region of the large electrical coupling, regardless of the increasing of the chemical coupling

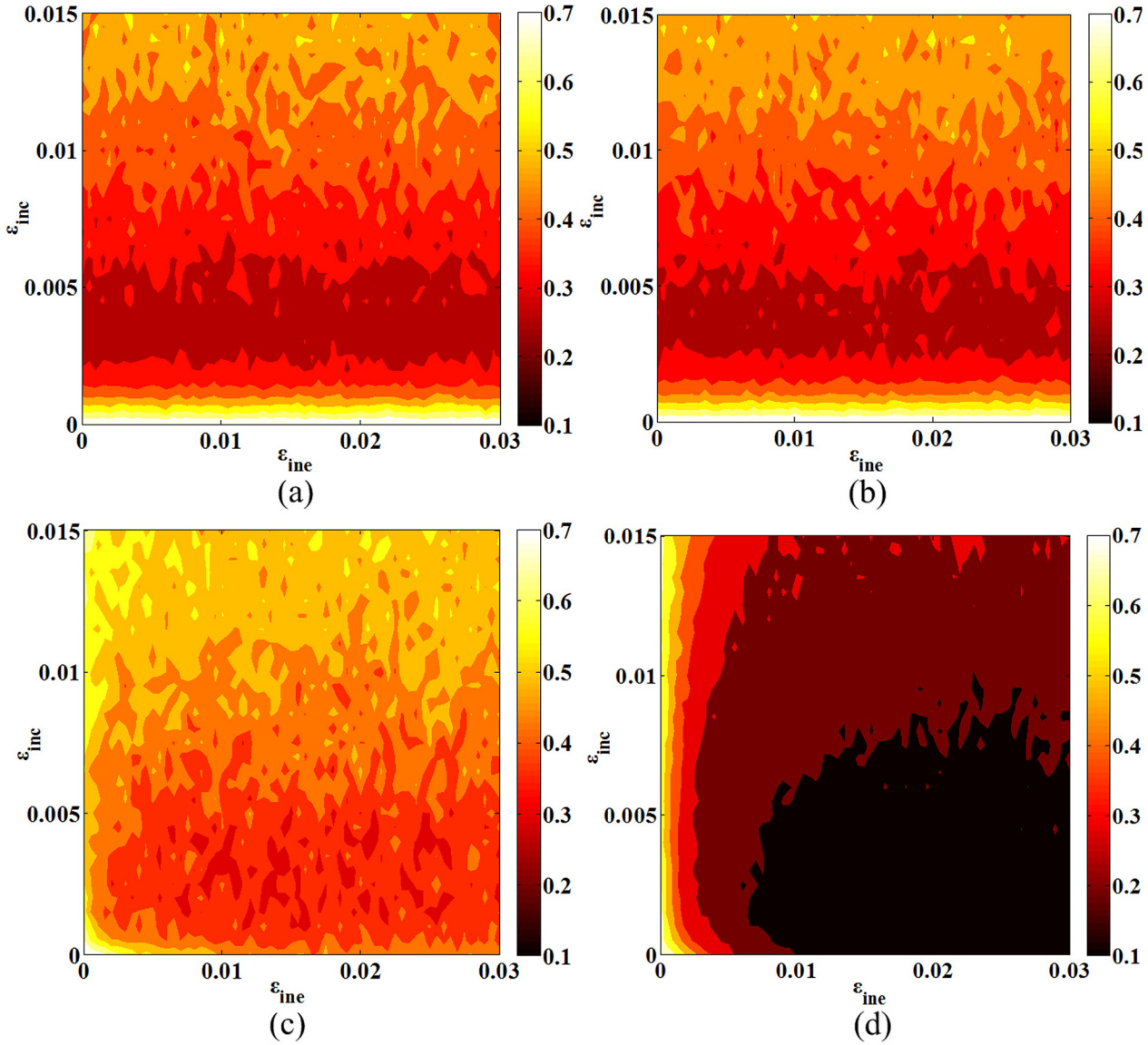


FIG. 12. Dependence of synchronization parameter $\sigma$ both on the electrical coupling strength $\varepsilon_{ine}$ and chemical coupling strength $\varepsilon_{inc}$. From (a) to (d), the probabilities of the electrical synapses are 0.2, 0.5, 0.7, and 0.8. Above a certain threshold of the electrical coupling's probability, the coupling strength of the electrical synapses starts to play an important role in the enhancement of the synchronous activities in neuronal ensemble.

strength. Here, a small quantity of chemical synapses seems to appear to have fewer impacts on synchronization transitions.

On the basis of the small-world properties exposed to the subnetworks of the modular neuronal network, the rewiring probability is a significant parameter to rebuild the structure of different subnetworks. The variations of the synchronization parameter $\sigma$ with respect to the probability of the electrical synapses $p$ for different values of rewiring probability $rp$ are plotted in the Fig. 13(a). It is shown that rewiring probability has less profound impact on the synchronous pattern, which implying the structure and the property of the subnetwork may seem less important. However, if only one subnetwork exists in the whole neuron system, rewiring probability can adjust the synchronization obviously, especially in the region of the small $rp$ where exhibit small-world property. As found in the Fig. 13(b), when the rewiring probability is smaller than the 0.4, the synchronous activities will be improved with the $rp$ increasing. While when the rewiring probability is above 0.4, synchronization can basically maintain invariable.

Finally, we further explore the dependence of the synchronization of the modular neuronal network on the clusters' number, as shown in Fig. 14. Here, the total number of neurons is limited to 200. Obviously, when the information transmission delay destroys synchronous activities of the neuronal population, such as $\tau = 400$, the number of the subnetworks seems have less profound impact on the synchronization. By contrast, in the regions of $\tau = 750$ that is an appropriate information transmission delay enhancing the emergence of the synchronous behaviors, large $M$ has a negative effect on the whole neuronal network's synchronization. Moreover, the relative positions of the lines which are marked by the circle and square respectively demonstrate that an increasing proportion of electrical synapses in the subnetwork can further improve the synchronous activities.

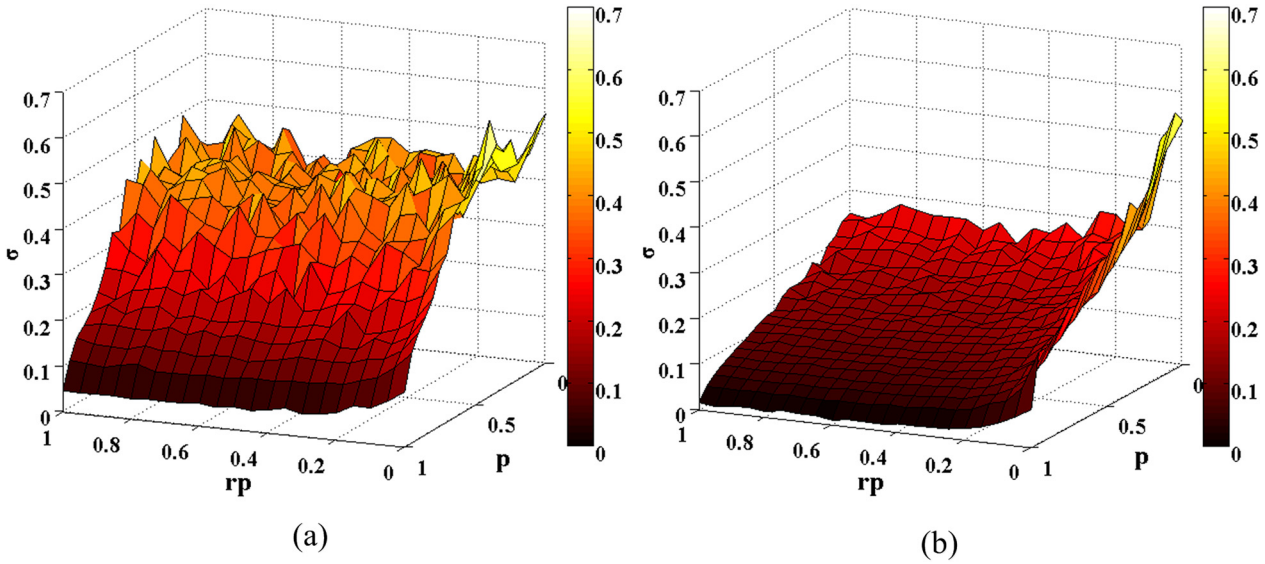


FIG. 13. 3D plots of the dependence of synchronization parameter $\sigma$ both on rewiring probability $rp$ and probability of the electrical synapses $p$ in the different neuronal networks. (a) The modular neuronal network with two small-world subnetworks. (b) The single small-world neuronal network. The property of the subnetwork such as rewiring probability seems to be more critical in the synchronization of the single module.

Overall inspections of the effect of $M$ and $\tau$ on $\sigma$ are described in Fig. 15, where panels (a) and (b) correspond to the probabilities of the electrical synapses being 0.8 and 0.5, respectively. Several band-like regions emerge, once more representing the synchronous activities of the neuronal ensemble. Interestingly, as $M$ increases, the regions of synchronization may turn narrow, which characterizes the synchronization of the modular neuronal network being gradually deteriorated. It implies the more dispersed the network structure, the more difficulties in coordinating with the neuronal activities in each belonging subnetwork.

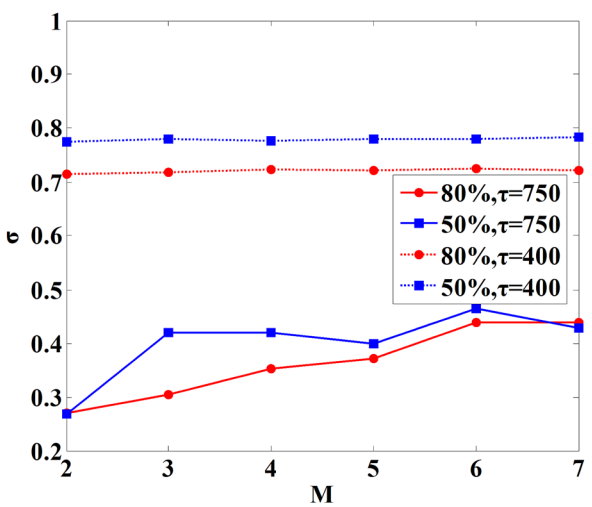


FIG. 14. Dependence of synchronization parameter $\sigma$ on the numbers of the subnetworks $M$ for different information transmission delays $\tau$ and probabilities of the electrical coupling. Other parameters are $\varepsilon_{in} = 0.01$, $\varepsilon_{ex} = 0.005$, and $rp = 0.1$. In the non-synchronization regions ($\tau = 400$), larger $\sigma$ have little fluctuations as the modules of the neuronal ensemble increased. In the synchronization regions ($\tau = 750$), increasing subnetworks reduce the synchronization, especially in the case of the large probability of the electrical synapses.

## IV. CONCLUSIONS

In this paper, the synchronization of spiking-bursting map-based neurons in the modular network with hybrid synapses has been studied. By merging all obtained observations about delay-induced synchronization transition, it is shown that intermittent transitions of synchronization can appear as the delay is varied, implying that information transmission delay always plays an important role in promoting or destroying synchronous neuronal activities. Interestingly, numerical results shows electrical coupling can enhance synchronous pattern in hybrid modular neuronal network with the small-world subnetworks, only if the probability of the electrical synapses achieves a certain level. Moreover, it can be found that coupling strength is a significant parameter which can largely influence the synchronous pattern. The results of the exploration demonstrate that the increasing intensive intra-synaptic coupling strength can radically enhance the synchronization of the networks. Besides, the intra-coupling strength of the subnetworks is further divided into the electrical coupling strength and the chemical coupling strength. Obtained results imply that the large coupling strength corresponding to large magnitude of synapses always promotes the synchronous activities in the modular network. Furthermore, it can be seen that large number of the subnetworks in the modular network can induce a detriment of the synchronized neuronal activities, which demonstrates that a large number of small clusters have poor coordination and synchronization.

As a result of the modular property in the coexistence of electrical and chemical synapses within the same networks and real neuronal networks, it is increasingly imperative to study modular neuronal networks with hybrid synapses. The presented results will be conducive for the further research on clinical diseases, such as Parkinson's tremor and epilepsy's rhythms. As expected, it has significant and meaningful implications for understanding the firing dynamics of neuronal networks.

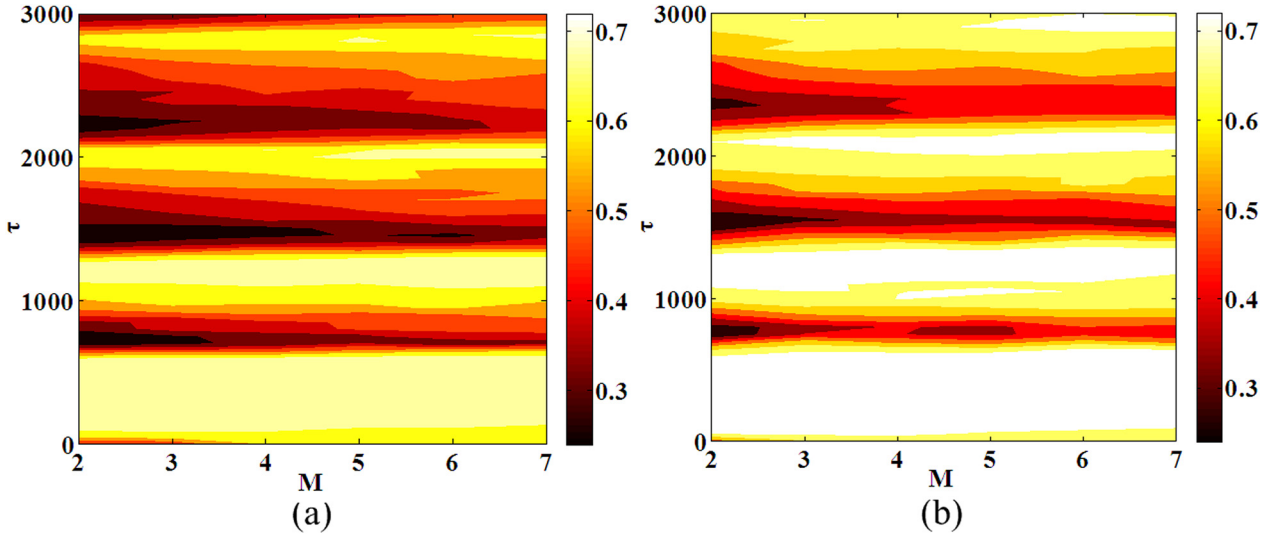


FIG. 15. Dependence of synchronization parameter $\sigma$ on the information transmission delays $\tau$ for different numbers of the subnetworks $M$. (a) The probability of the electrical synapses is 0.8. (b) The probability of the electrical synapses is 0.5. Other parameters are $\varepsilon_{in} = 0.01$, $\varepsilon_{ex} = 0.005$, and $rp = 0.1$. As $M$ increases, the regions of synchronization may turn narrow, which characterizes the synchronization of the modular neuronal network being gradually deteriorated.

## ACKNOWLEDGMENTS

This work was supported by the National Natural Science Foundation of China (Grant Nos. 61072012 and 61172009).

[1]E. Oh, K. Rho, H. Hong, and B. Kahng, Phys. Rev. E **72**, 047101 (2005).
[2]K. Park, Y. C. Lai, S. Gupte, and J. W. Kim, Chaos **16**, 015105 (2006).
[3]L. Huang, K. Park, Y. Lai, L. Yang, and K. Yang, Phys. Rev. Lett. **97**, 164101 (2006).
[4]Y. Tsukamoto, Y. Isomura, A. Nambu, and M. Takada, Neuroscience **119**, 265 (2003).
[5]S. Neuenschwander, M. Branco, and W. Singer, Vision Res. **39**, 2485 (1999).
[6]C. Gray, A. Engel, P. König, and W. Singer, Visual Neurosci. **8**, 337 (1992).
[7]A. Riehle, S. Grün, M. Diesmann, and A. Aertsen, Science **278**, 1950 (1997).
[8]P. Steinmetz, A. Roy, P. Fitzgerald, S. Hsiao, K. Johnson, and E. Niebur, Nature **404**, 187 (2000).
[9]P. Fries, P. Roelfsema, A. Engel, P. König, and W. Singer, Proc. Natl. Acad. Sci. U.S.A. **94**, 12699 (1997).
[10]R. Traub and R. Wong, Science **216**, 745 (1982).
[11]C. Babiloni, R. Ferri, D. Moretti, A. Stramb, G. Binetti, G. Forno, F. Ferreri, B. Lanuzza, C. Bonato, F. Nobili, G. Rodriguez, S. Salinari, S. Passero, R. Rocchi, C. Stam, and P. Rossini, Eur. J. Neurosci. **19**, 2583 (2004).
[12]A. Schnitzler and J. Gross, Nat. Rev. Neurosci. **6**, 285 (2005).
[13]J. Milton and P. Jung, *Epilepsy as a Dynamic Disease* (Springer-Verlag, Berlin, 2007).
[14]I. Leyva, I. Nadal, J. Almendral, and M. Sanjuán, Phys. Rev. E **74**, 056112 (2006).
[15]C. Liu, J. Wang, Y. Chen, B. Deng, and X. Wei, Int. J. Neural Syst. **23**, 1350017 (2013).
[16]W. Singer, Annu. Rev. Physiol. **55**, 349 (1993).
[17]I. Franović and V. Miljković, EPL **92**, 68007 (2010).
[18]L. Fernández, R. Huerta, F. Corbacho, and J. Sigüenza, Phys. Rev. Lett. **84**, 2758 (2000).
[19]P. Gade and C. Hu, Phys. Rev. E **62**, 6409 (2000).
[20]X. Wang and G. Chen, Int. J. Bifurcation Chaos Appl. Sci. Eng. **12**, 187 (2002).
[21]X. Wang and G. Chen, IEEE Trans. Circuits Syst. I **49**, 54 (2002).
[22]H. Hong, M. Choi, and B. Kim, Phys. Rev. E **65**, 026139 (2002).
[23]D. Watts and S. Strogatz, Nature **393**, 440 (1998).
[24]M. Barahona and L. Pecora, Phys. Rev. Lett. **89**, 054101 (2002).
[25]T. Nishikawa, A. Motter, Y. Lai, and F. Hoppensteadt, Phys. Rev. Lett. **91**, 014101 (2003).
[26]A. Barabási and R. Albert, Science **286**, 509 (1999).
[27]Q. Wang, G. Chen, and M. Perc, PloS ONE **6**, e15851 (2011).
[28]A. Motter, C. Zhou, and J. Kurths, Europhys Lett. **69**, 334 (2005).
[29]C. Zhou and J. Kurths, Phys. Rev. Lett. **96**, 164102 (2006).
[30]S. Wang, C. Hilgetag, and C. Zhou, Front. Comput. Neurosci. **5**, 30 (2011).
[31]O. Sporns, D. Chialvo, M. Kaiser, and C. Hilgetag, Trends Cogn. Sci. **8**, 418 (2004).
[32]C. Zhou, L. Zemanová, G. López, C. Hilgetag, and J. Kurths, New J. Phys. **9**, 178 (2007).
[33]E. Bullmore and O. Sporns, Nat. Rev. Neurosci. **10**, 186 (2009).
[34]C. Stam and J. Reijneveld, Nonlinear Biomed. Phys. **1**, 3 (2007).
[35]D. Meunier, R. Lambiotte, and E. Bullmore, Front. Neurosci. **4**, 200 (2010).
[36]G. Zamora-López, C. Zhou, and J. Kurths, Front. Neuroinform. **4**, 1 (2010).
[37]X. Sun, J. Lei, M. Perc, J. Kurths, and G. Chen, Chaos **21**, 016110 (2011).
[38]M. Newman, Proc. Natl. Acad. Sci. U.S.A. **98**, 404 (2001).
[39]Q. Wang, Z. Duan, M. Perc, and G. Chen, EPL **83**, 50008 (2008).
[40]J. Scannell, C. Blakemore, and M. Young, J. Neurosci. **15**, 1463 (1995).
[41]J. Scannell and M. Young, Curr. Biol. **3**, 191 (1993).
[42]C. Hilgetag, G. Burns, M. O'Neill, J. Scannell, and M. Young, Philos. Trans. R. Soc. London B **355**, 91 (2000).
[43]C. Hilgetag and M. Kaiser, Neuroinformatics **2**, 353 (2004).
[44]C. Liu, J. Wang, H. Yu, B. Deng, X. Wei, J. Sun, and Y. Chen, Chaos, Solitons Fractals **47**, 54 (2013).
[45]Y. Shen, Z. Hou, and H. Xin, Phys. Rev. E **77**, 031920 (2008).
[46]Q. Wang, A. Murks, M. Perc, and Q. Lu, Chin. Phys. B **20**, 040504 (2011).
[47]M. Galarreta and S. Hestrin, Nature **402**, 72 (1999).
[48]J. Gibson, M. Beierlein, and B. Connors, Nature **402**, 75 (1999).
[49]S. Hestrin and M. Galarreta, Trends Neurosci. **28**, 304 (2005).
[50]M. Galarreta and S. Hestrin, Nat. Rev. Neurosci. **2**, 425 (2001).
[51]B. Connors and M. Long, Annu. Rev. Neurosci. **27**, 393 (2004).
[52]M. Bennett, Brain Res. Rev. **32**, 16 (2000).
[53]S. Hestrin, Science **334**, 315 (2011).
[54]P. Greengard, Science **294**, 1024 (2001).
[55]N. Kopell and B. Ermentrout, Proc. Natl. Acad. Sci. U.S.A. **101**, 15482 (2004).
[56]M. Baptista, F. Kakmeni, and C. Grebogi, Phys. Rev. E **82**, 036203 (2010).
[57]E. Kandel, J. Schwartz, and T. Jessell, *Principles of Neural Science* (Elsevier, Amsterdam, 1991).
[58]A. Roxin, N. Brunel, and D. Hansel, Phys. Rev. Lett. **94**, 238103 (2005).
[59]M. Gosak, R. Markovic, and M. Marhl, Physica A **391**, 2764 (2012).

[60]Q. Wang, M. Perc, Z. Duan, and G. Chen, Chaos **19**, 023112 (2009).
[61]Q. Wang and G. Chen, Chaos **21**, 013123 (2011).
[62]H. Yu, J. Wang, Q. Liu, J. Sun, and H. Yu, Chaos, Solitons Fractals **48**, 68 (2013).
[63]Q. Wang, M. Perc, Z. Duan, and G. Chen, Physica A **389**, 3299 (2010).
[64]Q. Wang, M. Perc, Z. Duan, and G. Chen, Phys. Rev. E **80**, 026206 (2009).
[65]N. Rulkov, Phys. Rev. E **65**, 041922 (2002).
[66]N. Rulkov, Phys. Rev. Lett. **86**, 183 (2001).
[67]T. Ko and G. Ermentrout, Phys. Rev. E **76**, 056206 (2007).